THE JOURNAL OF PHYSICAL CHEMISTRY A

ARTICLE

pubs.acs.org/JPCA

Atmospheric Chemistry of (*Z*)-$CF_3CH{=}CHCF_3$: OH Radical Reaction Rate Coefficient and Global Warming Potential

Munkhbayar Baasandorj,[†,‡] A.R. Ravishankara,[†] and James B. Burkholder*[,†]

[†]Earth System Research Laboratory, Chemical Sciences Division, National Oceanic and Atmospheric Administration, 325 Broadway, Boulder, Colorado 80305-3328, United States

[‡]Cooperative Institute for Research in Environmental Sciences, University of Colorado, Boulder, Colorado 80309, United States

Supporting Information

ABSTRACT: Rate coefficients, *k*, for the gas-phase reaction of the OH radical with (*Z*)-$CF_3CH{=}CHCF_3$ (*cis*-1,1,1,4,4,4-hexafluoro-2-butene) were measured under pseudo-first-order conditions in OH using pulsed laser photolysis (PLP) to produce OH and laser-induced fluorescence (LIF) to detect it. Rate coefficients were measured over a range of temperatures (212−374 K) and bath gas pressures (20−200 Torr; He, N_2) and found to be independent of pressure over this range of conditions. The rate coefficient has a non-Arrhenius behavior that is well-described by the expression $k_1(T) = (5.73 \pm 0.60) \times 10^{-19} \times T^2 \times \exp[(678 \pm 10)/T]$ cm^3 molecule^{-1} s^{-1} where k_1(296 K) was measured to be $(4.91 \pm 0.50) \times 10^{-13}$ cm^3 molecule^{-1} s^{-1} and the uncertainties are at the 2σ level and include estimated systematic errors. Rate coefficients for the analogous OD radical reaction were determined over a range of temperatures (262−374 K) at 100 Torr (He) to be $k_2(T) = (4.81 \pm 0.20) \times 10^{-19} \times T^2 \times \exp[(776 \pm 15)/T]$, with $k_2(296\ \text{K}) = (5.73 \pm 0.50) \times 10^{-13}$ cm^3 molecule^{-1} s^{-1}. OH radical rate coefficients were also measured at 296, 345, and 375 K using a relative rate technique and found to be in good agreement with the PLP−LIF results. A room-temperature rate coefficient for the O_3 + (*Z*)-$CF_3CH{=}CHCF_3$ reaction was measured using an absolute method with O_3 in excess to be $<6 \times 10^{-21}$ cm^3 molecule^{-1} s^{-1}. The atmospheric lifetime of (*Z*)-$CF_3CH{=}CHCF_3$ due to loss by OH reaction was estimated to be ∼20 days. Infrared absorption spectra of (*Z*)-$CF_3CH{=}CHCF_3$ measured in this work were used to determine a (*Z*)-$CF_3CH{=}CHCF_3$ global warming potential (GWP) of ∼9 for the 100 year time horizon. A comparison of the OH reactivity of (*Z*)-$CF_3CH{=}CHCF_3$ with other unsaturated fluorinated compounds is presented.

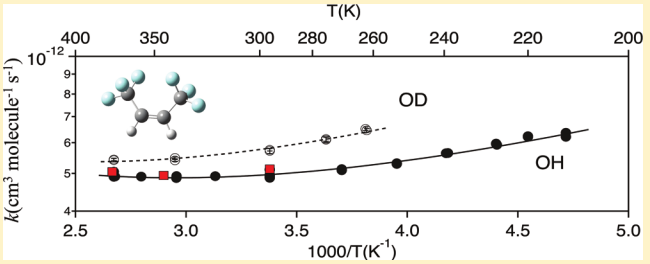

1. INTRODUCTION

The Montreal Protocol (1987), and its subsequent adjustments and amendments, has led to the commercial replacement of ozone-depleting substances (ODS), including chlorofluorocarbons (CFCs) and bromofluorocarbons (halons), with hydrochlorofluorocarbons (HCFCs) and hydrofluorocarbons (HFCs) in many cases. CFCs now exhibit substantially reduced rates of atmospheric growth, and a decline in the atmospheric abundance of some compounds has been observed. The atmospheric abundances of HCFCs and HFCs, on the other hand, are generally increasing.[1] HCFCs are considered to be transitional replacements and are scheduled for phase-down under the Montreal Protocol.[1,2] HFCs are not ozone-depleting compounds but are potent greenhouse gases that are included under the Kyoto Protocol (1997).[3] The radiative forcing due to HFCs is projected to increase as the use of HFCs increases, with a potentially significant contribution to climate forcing.[4] It is, therefore, important that HFC replacement compounds and their atmospheric degradation products have acceptably low global warming potentials (GWPs) in addition to having a negligible impact on the environment, for example, low photochemical ozone-creation potentials (POCP).

Unsaturated hydrofluorocarbons (HFOs, hydrofluoro-olefins) are currently being considered as viable replacement compounds due in part to their greater reactivity in the atmosphere with the OH radical than the HFCs that they replace, which results in shorter atmospheric lifetimes. A shorter atmospheric lifetime in most cases leads to a lower GWP for HFOs compared to that for the HFCs that they replace. (*Z*)-$CF_3CH{=}CHCF_3$ (*cis*-1,1,1,4,4,4-hexafluoro-2-butene) is a potential replacement compound currently under consideration. Prior to its use in commercial applications and possible release into the atmosphere, its atmospheric chemistry and potential impact on the environment need to be understood. The primary atmospheric loss process for (*Z*)-$CF_3CH{=}CHCF_3$ is expected to be reaction with the OH radical

$$\text{OH} + (Z)\text{-}CF_3CH{=}CHCF_3 \rightarrow \text{Products} \qquad (1)$$

Analogous to other alkene reactions, reaction 1 is expected to proceed via addition to the carbon−carbon double bond, resulting in the formation of a stable HO−HFC adduct radical.

Received: June 30, 2011
Revised: August 11, 2011
Published: September 01, 2011

In the atmosphere, the HO−HFC adduct would, most likely, react with O_2, leading to the irreversible removal of (*Z*)-$CF_3CH{=}CHCF_3$.

In this study, rate coefficients for reaction 1, $k_1(T)$, were measured as a function of temperature (212−374 K) and pressure (20−200 Torr, He, N_2) using a pulsed laser photolysis−laser induced fluorescence (PLP−LIF) technique and at 296, 345, and 375 K using a relative rate (RR) technique at pressures between 100 and 300 Torr (He). To our knowledge, rate coefficient studies for reaction 1 have not been reported in the literature to date. Rate coefficients for the OD reaction

$$\text{OD} + (Z)\text{-}CF_3CH{=}CHCF_3 \rightarrow \text{Products} \quad (2)$$

were also measured as part of this study to gain additional insight into the mechanism of reaction 1. A comparison of the (*Z*)-$CF_3CH{=}CHCF_3$ reactivity with that of other unsaturated fluorinated compounds is presented. The reaction of (*Z*)-$CF_3CH{=}CHCF_3$ with O_3 was briefly examined and shown to represent only a minor atmospheric loss process. The radiative efficiency and global warming potential of (*Z*)-$CF_3CH{=}CHCF_3$ were calculated using its infrared absorption spectrum measured as part of this work.

2. EXPERIMENTAL DETAILS

The pulsed PLP−LIF[5,6] and RR[7,8] apparatus have been used previously in our laboratory, and only details relevant to the present study are described separately below. Measurements of the O_3 + (*Z*)-$CF_3CH{=}CHCF_3$ reaction rate coefficient at 296 K and the infrared absorption cross sections of (*Z*)-$CF_3CH{=}CHCF_3$ are described in sections 2.3 and 2.4, respectively.

2.1. Pulsed Laser Photolysis−Laser-Induced Fluorescence (PLP−LIF). Reaction rate coefficients were measured under pseudo-first-order conditions in OH, [HFO] ≫ [OH], with OH radicals produced via the 248 nm (KrF excimer laser) pulsed laser photolysis of H_2O_2 (hydrogen peroxide) or $(CH_3)_3COOH$ (*t*-butyl hydroperoxide)

$$H_2O_2 + h\nu \rightarrow 2\text{OH} \quad (3)$$

$$(CH_3)_3COOH + h\nu \rightarrow \text{product} + \text{OH} \quad (4)$$

where the OH quantum yield for reaction 3 is 2[9] and that for reaction 4 is unity.[10] H_2O_2 photolysis was used for kinetic measurements at temperatures > 250 K. For temperatures < 250 K, $(CH_3)_3COOH$ photolysis was used. Details of the $(CH_3)_3COOH$ photolysis OH radical source are provided in a recent study from this laboratory.[10] The initial OH radical concentration, $[OH]_0$, was estimated from the precursor concentration, its absorption cross section at 248 nm, the precursor OH quantum yield, and the photolysis laser power, which was measured at the exit of the LIF reactor with a calibrated power meter. The photolysis laser fluence was varied between 3 and 17 mJ cm^{-2} $pulse^{-1}$ over the course of the study. The concentrations of H_2O_2 and $(CH_3)_3COOH$ in the LIF reactor were estimated from the pseudo-first-order rate coefficients measured in the absence of (*Z*)-$CF_3CH{=}CHCF_3$.

The temperature of the ∼150 cm^3 Pyrex LIF reactor was controlled by circulating fluid from a temperature-regulated reservoir through its jacket. The temperature of the gas in the reactor was measured with a retractable thermocouple and was accurate to within ±1 K.

OD radicals were produced using 248 nm pulsed laser photolysis of O_3 in a He bath gas to produce $O(^1D)$ followed by its reaction with D_2O

$$O(^1D) + D_2O \rightarrow 2\text{OD} \quad (5)$$

The D_2O concentration was estimated from gas flow rates and pressures to be ∼3×10^{16} molecules cm^{-3}, which is sufficient to remove 99% of the $O(^1D)$ within 1 μs after the photolysis pulse and quench the vibrationally excited OD produced in reaction 5 within 15 μs.[11] The O_3 concentration in the LIF reactor was estimated to be ∼4×10^{12} molecules cm^{-3}.

OH radical fluorescence was detected following pulsed laser excitation in the $A^2\Sigma^+(v = 1) \leftarrow X^2\Pi(v = 0)$ transition near 282 nm using the frequency-doubled output from a Nd:YAG pumped dye laser. OD fluorescence was detected following excitation near 287.6 nm. The probe laser beam propagated through the LIF reactor at a right angle to the larger diameter photolysis laser beam. The photolysis and probe beams intersected in the middle of the reactor. Fluorescence from the reaction zone was detected by a photomultiplier tube (PMT) mounted orthogonal to the plane of the photolysis and probe laser beams. A band-pass filter (308 nm, fwhm =10 nm) mounted in front of the PMT was used to isolate the OH fluorescence. The PMT signal was averaged for 100 laser shots with a gated charge integrator. OH temporal profiles were measured by varying the delay between the photolysis and the probe lasers (i.e., the reaction time) between 10 μs and 50 ms.

OH temporal profiles followed the integrated first-order rate expression

$$\ln\left(\frac{[OH]_t}{[OH]_0}\right) = \ln\left(\frac{S_t}{S_0}\right) = -(k_1[(Z)\text{-}CF_3CH{=}CHCF_3] + k_d)t = -k't \quad (I)$$

where S_t is the measured OH signal at time *t*, which is proportional to $[OH]_t$, $[(Z)\text{-}CF_3CH{=}CHCF_3]$ is the (*Z*)-$CF_3CH{=}CHCF_3$ concentration in the LIF reactor, and k' and k_d are the first-order rate coefficients for loss of OH in the presence and absence of (*Z*)-$CF_3CH{=}CHCF_3$, respectively. The k' values were obtained as the slope of a nonlinear least-squares fit of S_t versus time. k_d represents the loss of OH due primarily to its reaction with the OH precursor and diffusion out of the detection volume. The actual values of k_d depended on the OH radical precursor and its concentration but were in the range of 50−500 s^{-1}. OH temporal profiles were measured over a range of (*Z*)-$CF_3CH{=}CHCF_3$ concentrations at each temperature and pressure. Rate coefficients, $k_1(T)$, were determined as the slope of k' versus $[(Z)\text{-}CF_3CH{=}CHCF_3]$ using a linear least-squares fit of the data weighted by the measurement precision.

2.2. Relative Rate (RR) Measurements. In the RR method, the loss of the reactant compound, (*Z*)-$CF_3CH{=}CHCF_3$, was measured relative to the loss of a reference compound that has a well-established reaction rate coefficient. Provided the reactant and reference compounds are lost via the same reaction, in this case, reaction with the OH radical, the rate coefficients for the two reactions are related by

$$\ln\left(\frac{[(Z)\text{-}CF_3CH{=}CHCF_3]_0}{[(Z)\text{-}CF_3CH{=}CHCF_3]_t}\right) = \frac{k_Z}{k_{Ref}}\ln\left(\frac{[Ref]_0}{[Ref]_t}\right) \quad (II)$$

where the 0 and t subscripts indicate the initial concentrations at time zero and concentrations during the reaction at time t. The k_Z and k_{Ref} are the rate coefficients for the (Z)-$CF_3CH{=}CHCF_3$ and reference reaction with OH. C_2H_6 was used as the reference compound, where $k(T) = 7.66 \times 10^{-12} \exp[-1020/T]$ cm^3 molecule^{-1} s^{-1} and $k(296\ K) = (2.50 \pm 0.23) \times 10^{-13}$ cm^3 molecule^{-1} s^{-1} for the OH + C_2H_6 reaction.[9] Several experiments were performed using CH_3CH_2Cl as a reference compound. However, the use of CH_3CH_2Cl led to systematic deviations due to secondary loss of (Z)-$CF_3CH{=}CHCF_3$, which was most noticeable at reactant losses > 20%. HCl formation was observed during the experiment, suggesting a possible interference from Cl atom reactions. A rate coefficient obtained using data obtained with small reactant conversion was, however, found to be in agreement with the results obtained using C_2H_6 as the reference compound. The results obtained in the CH_3CH_2Cl experiments were not used in the final kinetic analysis due to the possible contributions of systematic errors in the measurements.

The apparatus used for the RR measurements has been described in detail elsewhere.[7,8] The apparatus consisted of a 100 cm long reaction cell (5 cm i.d.) coupled to a Fourier trans form infrared spectrometer (FTIR) for measuring the reactant concentrations. OH radicals were produced using the 248 nm pulsed laser photolysis of O_3 in a He bath gas to produce $O(^1D)$ followed by its reaction with H_2O

$$O(^1D) + H_2O \rightarrow 2OH \qquad (6)$$

Experiments were performed by first filling the reactor with (Z)-$CF_3CH{=}CHCF_3$, reference compound, H_2O vapor, and ~100 Torr He bath gas. The gases were thoroughly mixed using a Teflon diaphragm circulation pump. The (Z)-$CF_3CH{=}CHCF_3$ and reference compound concentrations were then measured by infrared absorption. Ozone was then slowly added to the circulating gas mixture by passing a small flow of He through the O_3 reservoir while the photolysis laser beam was passed along the length of the reactor. The residence time of the gas in the reaction cell was ~6 s. The steady-state O_3 concentration was estimated to be $\sim 1 \times 10^{14}$ molecules cm^{-3}. The H_2O vapor concentration was estimated to be $\sim 4 \times 10^{17}$ molecules cm^{-3}, which was sufficient to scavenge >99% of the $O(^1D)$ atoms, that is, the loss of (Z)-$CF_3CH{=}CHCF_3$ or C_2H_6 due to reaction with $O(^1D)$ was estimated to be <0.3 or <1% (worst case), respectively, of their measured loss. The total pressure of the system increased due to the addition of O_3/He during the experiment from 100 to ~200 Torr over the duration of an experiment.

The reactant and reference compound loss was measured by infrared absorption. Infrared spectra were recorded at a spectral resolution of 1 cm^{-1} between 500 and 4000 cm^{-1} with 20 co-added interferograms. The losses of C_2H_6 and (Z)-$CF_3CH{=}CHCF_3$ were monitored using the absorption bands near 820 and 3000 cm^{-1} and bands between 1000 and 1500 cm^{-1}, respectively. In dark experiments, performed under identical conditions but without the photolysis laser beam, there was no observable change, <0.5%, in the reactant concentrations over a period of 2 h with a pressure increase from 100 to 500 Torr (He).

The photolysis laser fluence was measured at the exit of the reactor with a power meter and was constant to within 5% during an experiment but was varied over the range of 12−26 mJ cm^{-2} pulse^{-1} over the course of the study. The initial concentrations were varied in the individual experiments with values in the range of $(6-13) \times 10^{14}$ molecules cm^{-3} for (Z)-$CF_3CH{=}CHCF_3$ and $(0.5-10) \times 10^{15}$ molecules cm^{-3} for C_2H_6. Several experiments were also performed with O_2, $\sim 7 \times 10^{16}$ molecules cm^{-3}, added to the initial reaction mixture to test for possible contributions from secondary radical chemistry.

2.3. O_3 + (Z)-$CF_3CH{=}CHCF_3$ Rate Coefficient. The room-temperature rate coefficient for the reaction of O_3 with (Z)-$CF_3CH{=}CHCF_3$ was measured under static conditions at pressures between 100 and 250 Torr (He) using infrared absorption to monitor the loss of (Z)-$CF_3CH{=}CHCF_3$ in the presence of excess O_3. Rate coefficients were measured under pseudo-first-order conditions in (Z)-$CF_3CH{=}CHCF_3$, $[O_3] \gg [(Z)\text{-}CF_3CH{=}CHCF_3]$, and interpreted assuming that the observed (Z)-$CF_3CH{=}CHCF_3$ loss was due solely to its reaction with O_3. Experiments were performed using the same apparatus setup used in the OH RR measurements described above. Several experiments were performed using the multipass infrared absorption cell as the reactor, that is, without circulation of the gases. The O_3 concentration was varied over the range of $(1.9-8.6) \times 10^{16}$ molecules cm^{-3} during the course of the study and was quantified using its infrared absorption band near 2100 cm^{-1}.[12] The (Z)-$CF_3CH{=}CHCF_3$ concentration was in the range of $(3.9-7.5) \times 10^{14}$ molecules cm^{-3} with $[O_2]$ in the range of $(0.5-10) \times 10^{16}$ molecules cm^{-3}. Rate coefficients were obtained from a linear least-squares fit of the measured pseudo-first-order rate coefficients versus $[O_3]$.

2.4. UV and Infrared Absorption Measurements. UV (184.9 and 253.6 nm) and infrared absorption cross sections of (Z)-$CF_3CH{=}CHCF_3$ were determined in this work and used in monitoring its concentration online in the PLP−LIF kinetic measurements, measuring the rate coefficient of the O_3 + (Z)-$CF_3CH{=}CHCF_3$ reaction, as well as in the determination of its GWPs. Absorption cross sections were determined at room temperature, 296 K, and were based on absolute pressure measurements made under static conditions with manometrically prepared mixtures of (Z)-$CF_3CH{=}CHCF_3$ (0.7 and 8% in He) as well as pure samples.

UV absorption was measured using a Hg pen-ray lamp light source, a 100 cm long absorption cell, and a band-pass filter mounted in front of a photodiode detector (solar blind detector for 185 nm). Absorption cross sections were determined from measurements made over a range of (Z)-$CF_3CH{=}CHCF_3$ concentrations using Beer's Law

$$A = -\ln\left(\frac{I}{I_0}\right) = \sigma L[(Z)\text{-}CF_3CH{=}CHCF_3] \qquad (III)$$

where I and I_0 are the transmitted intensity through the cell with and without (Z)-$CF_3CH{=}CHCF_3$ present, respectively, σ is the (Z)-$CF_3CH{=}CHCF_3$ absorption cross section, and L is the path length of the absorption cell. The range of (Z)-$CF_3CH{=}CHCF_3$ concentrations used was $(0.78-3.70) \times 10^{16}$ molecules cm^{-3} for 184.9 nm and $(0.1-1) \times 10^{19}$ molecules cm^{-3} for 253.6 nm. A linear least-squares analysis of A versus $[(Z)\text{-}CF_3CH{=}CHCF_3]$ yielded a 184.9 nm absorption cross section of $(4.97 \pm 0.02) \times 10^{-19}$ cm^2 molecule^{-1}, where the quoted uncertainties are at the 2σ level from the precision of the fit, eq III. Absorption cross sections obtained using different sample mixtures were identical within the precision of the measurement. For 253.6 nm, a cross section upper-limit of $<4 \times 10^{-24}$ cm^2 molecule^{-1} was determined. In the kinetic experiments, UV absorption of (Z)-$CF_3CH{=}CHCF_3$ at 184.9 nm was measured before the sample entered the LIF reactor.

Table 1. Summary of Experimental Conditions and Rate Coefficients Obtained For the OH + (*Z*)-$CF_3CH{=}CHCF_3$ Reaction

T (K)	P (Torr)	bath gas	$[O_2]$ (10^{16} molecules cm^{-3})	v (cm s^{-1})	photolysis laser fluence (mJ cm^{-2} $pulse^{-1}$)	[precursor] (10^{14} molecules cm^{-3})	$[OH]_0$ (10^{11} molecules cm^{-3})	[Z-$CF_3CH{=}CHCF_3$] (10^{15} molecules cm^{-3})	k^c (10^{-13} cm^3 $molecule^{-1}$ s^{-1})
212	200	He		6.9	10.4	0.86[a]	0.22	0.88−13.3	6.36 ± 0.10
212	200	He		7.5	10.7	0.87[a]	0.23	0.53−15.5	6.21 ± 0.05
212	200	He	3.6	7.5	10.7	0.87[a]	0.23	0.53−15.5	6.21 ± 0.08
									k(212 K) = 6.26 ± 0.06[d]
220	200	He		7.7	10.7	0.69[a]	0.18	0.58−11.7	6.23 ± 0.08
220	200	N_2		6.6	11	0.71[a]	0.19	0.80−15.8	6.21 ± 0.10
220	200	N_2	4.05	6.6	11	0.71[a]	0.19	0.95−15.7	6.21 ± 0.11
									k(220 K) = 6.21 ± 0.06[d]
227	200	He		6.5	11.4	1.01[a]	0.29	0.97−16.3	5.96 ± 0.08
227	200	He	4.20	6.5	11.4	1.01[a]	0.29	0.68−15.4	5.97 ± 0.05
227	200	N_2		6.8	10.4	1.02[a]	0.30	0.75−14.9	5.92 ± 0.08
									k(227 K) = 5.96 ± 0.03[d]
239	100	He		9.6	9.4	1.73[a]	0.41	0.91−14.4	5.63 ± 0.04
239	200	He		6.6	15.9	1.04[a]	0.41	0.88−14.5	5.64 ± 0.06
									k(239 K) = 5.63 ± 0.04[d]
253	200	He		6.9	11.9	0.35[b]	0.94	1.15−18.1	5.29 ± 0.04
253	100	N_2		8.6	14.8	1.47[b]	4.86	0.80−12.8	5.31 ± 0.05
									k(253 K) = 5.30 ± 0.04[d]
270	200	He		7.4	11.9	0.34[b]	0.92	0.80−16.5	5.09 ± 0.04
270	200	He		7.4	11.9	0.34[b]	0.92	0.42−13.3	5.13 ± 0.07
									k(270 K) = 5.11 ± 0.04[d]
296	50	He		12.3	15.1	0.96[b]	3.26	0.36−17.3	4.95 ± 0.03
296	100	He		11.9	16.7	0.59[b]	2.21	0.53−6.5	5.12 ± 0.08
296	100	He		15.7	7.0	0.97[b]	1.52	0.39−13.0	4.89 ± 0.05
296	100	He	1.2	11.8	9.4	1.64[a]	0.39	0.72−15.3	4.88 ± 0.04
296	200	He		7.8	17.4	0.22[b]	0.88	2.23−24.5	5.11 ± 0.04
296	200	He		7.8	15.8	0.43[b]	1.54	0.65−17.2	4.92 ± 0.07
296	200	He	3.39	7.8	15.8	0.43[b]	1.54	0.57−19.1	4.87 ± 0.03
296	100	N_2		7.6	6.3	2.01[b]	2.87	0.52−18.0	4.92 ± 0.04
296	100	N_2	3.64	7.6	6.3	2.01[b]	2.87	0.51−18.4	4.94 ± 0.08
									k(296 K) = 4.91 ± 0.02[d]
319	200	He		7.9	8.6	0.53[b]	1.02	0.40−16.2	4.92 ± 0.04
338	200	He		8.1	8.6	0.66[b]	1.27	1.18−16.0	4.86 ± 0.02
338	200	N_2		8.0	14.7	0.55[b]	1.83	0.97−21.2	4.90 ± 0.04
338	200	N_2		8.0	14.7	0.55[b]	1.83	0.92−18.5	4.92 ± 0.05
									k(338 K) = 4.88 ± 0.02[d]
357	200	He		8.6	8.6	0.67[b]	1.29	0.51−13.7	4.90 ± 0.03
374	24	He		14	14.3	0.40[b]	1.27	0.33−11.4	5.05 ± 0.09

dx.doi.org/10.1021/jp206195g | *J. Phys. Chem. A* 2011, 115, 10539–10549

Table 1. Continued

T (K)	P (Torr)	bath gas	$[O_2]$ (10^{16} molecules cm^{-3})	v (cm s^{-1})	photolysis laser fluence (mJ cm^{-2} pulse^{-1})	[precursor] (10^{14} molecules cm^{-3})	$[OH]_0$ (10^{11} molecules cm^{-3})	[Z-$CF_3CH{=}CHCF_3$] (10^{15} molecules cm^{-3})	k^c (10^{-13} cm^3 molecule^{-1} s^{-1})
374	200	He		8.6	15.1	0.40	1.34[b]	0.46−18.1	4.94 ± 0.03
374	200	He	3.13	8.6	15.1	0.40	1.34[b]	0.76−17.2	4.90 ± 0.04
374	50	N_2		9.8	17.3	0.93	3.60[b]	0.80−16.0	4.94 ± 0.04
374	50	N_2	2.72	10	17.3	0.93	3.60[b]	0.23−11.4	4.92 ± 0.04
									k(374 K) = 4.94 ± 0.05[d]

[a] $(CH_3)_3COOH$ was used as the OH precursor. [b] H_2O_2 was used as the OH source. [c] The quoted uncertainties are the 2σ precision from the linear least-squares fit of k' versus [(*Z*)-$CF_3CH{=}CHCF_3$]. [d] Determined from a weighted linear least-squares fit to all ($k' - k_d$) versus [(*Z*)-$CF_3CH{=}CHCF_3$].

Table 2. Summary of Experimental Conditions and Rate Coefficients Obtained for the OD + (*Z*)-$CF_3CH{=}CHCF_3$ Reaction

T (K)	P (Torr, He)	$[O_2]$ (10^{16} molecules cm^{-3})	v (cm s^{-1})	photolysis laser fluence (mJ cm^{-2} pulse^{-1})	$[O_3]$ (10^{12} molecules cm^{-3})	$[D_2O]$ (10^{16}molecules cm^{-3})	$[OH]_0$ (10^{11} molecules cm^{-3})	[Z-$CF_3CH{=}CHCF_3$] (10^{15} molecules cm^{-3})	k^a (10^{-13} cm^3 molecule^{-1} s^{-1})
262	100		9.0	5.6	3.83	3.06	5.7	0.38−13.7	6.51 ± 0.07
262	100	3.08	9.0	5.6	3.83	3.06	5.7	0.38−14.1	6.45 ± 0.07
									k(262 K) = 6.47 ± 0.06[b]
275	100		8.8	8.1	3.91	3.11	8.4	0.56−15.1	6.10 ± 0.09
275	100	3.13	8.8	8.1	3.91	3.11	8.4	0.46−15.4	6.13 ± 0.08
									k(275 K) = 6.11 ± 0.07[b]
296	100		10.2	5.7	3.34	2.73	5.1	0.33−14.9	5.71 ± 0.09
296	100	2.70	10.2	5.7	3.34	2.73	5.1	0.42−13.6	5.75 ± 0.04
									k(296 K) = 5.73 ± 0.07[b]
339	100		11.8	5.6	4.2	2.38	6.5	0.53−16.2	5.48 ± 0.03
339	100	2.35	11.8	5.6	4.2	2.38	6.5	0.89−14.1	5.40 ± 0.03
									k(339 K) = 5.46 ± 0.04[b]
374	100		12.8	5.7	2.71	2.17	4.1	0.32−18.2	5.41 ± 0.05
374	100	2.20	12.8	5.7	2.71	2.17	4.1	0.29−16.0	5.43 ± 0.04
									k(374 K) = 5.41 ± 0.04[b]

[a] The quoted uncertainties are at the 2σ level from the precision of the fit. [b] Determined from a weighted linear least-squares fit of all ($k' - k_d$) data versus concentration.

dx.doi.org/10.1021/jp206195g | J. Phys. Chem. A 2011, 115, 10539–10549

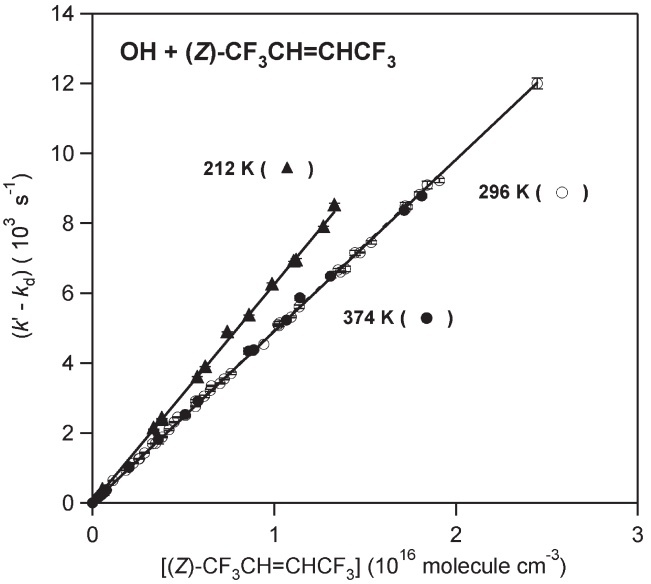

Figure 1. Pseudo-first-order rate coefficient data for the reaction of OH with (*Z*)-$CF_3CH{=}CHCF_3$ at 296 K and the temperature extremes included in this study, 212 and 374 K. The lines are linear least-squares fits of the data to eq I.

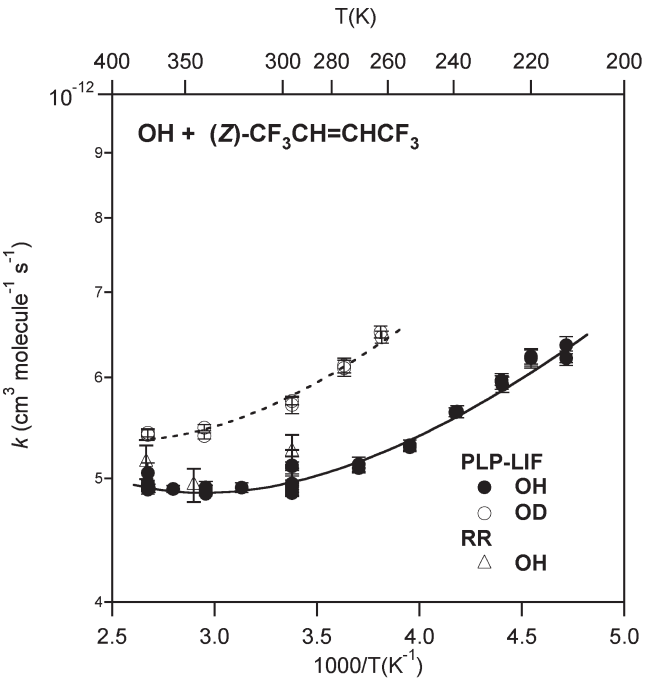

Figure 2. Temperature dependence of the rate coefficients for the OH and OD reactions with (*Z*)-$CF_3CH{=}CHCF_3$: OH reaction (filled circles), pulsed laser photolysis−laser induced fluorescence (PLP−LIF) technique (circles), and relative rate technique (RR) (triangles); OD reaction (open circles) obtained using the PLP−LIF technique. The PLP−LIF and RR data include the 2σ uncertainty from the precision of the measurements. The lines are the least-squares fits of the PLP−LIF data to the expression $k(T) = AT^2 \exp(-E/RT)$.

Infrared absorption spectra were recorded using a FTIR equipped with a low-volume multipass absorption cell (750 cm^3, 485 cm optical path length). Spectra were measured between 500 and 4000 cm^{-1} with a spectral resolution of 1 cm^{-1}. During the PLP−LIF kinetic experiments, infrared absorption measurements were made either before or after the LIF reactor.

2.5. Materials. He (UHP, 99.999%), N_2 (UHP, 99.99%), N_2 (UHP, O_2 < 0.5 ppm), and O_2 (UHP, 99.99%) were used as supplied. Concentrated H_2O_2 (>95% mole fraction) was prepared by bubbling N_2 for several days through a sample that was initially ~60% mole fraction. The $(CH_3)_3COOH$ sample (70 wt% in H_2O) was obtained commercially. H_2O_2 and $(CH_3)_3COOH$ were introduced into the gas flow by passing a small flow of He through a bubbler containing the liquid samples. The gas-phase composition from the $(CH_3)_3COOH$ sample was approximately 56% $(CH_3)_3COOH$ and 44% H_2O.[10] H_2O_2 and $(CH_3)_3COOH$ were added to the main gas flow just prior to entering the LIF reactor.

(*Z*)-$CF_3CH{=}CHCF_3$ (99.95%) samples were degassed in several freeze−pump−thaw cycles before use. The (*Z*)-$CF_3CH{=}CHCF_3$ sample was analyzed using gas chromatography and found to include the following minor impurities: (*E*)-$CF_3CH{=}CHCF_3$ (0.0037 wt %), (*Z*)-2-chloro-1,1,1,4,4,4-hexafluoro-2-butene (0.0001 wt%), (*E*)-1,1,1,4,4-pentafluoro-2-butene (0.0059%), (*Z*)-1-chloro-1,1,4,4,4-pentafluoro-2-butene (0.0019%), and saturated fluorocarbons (0.0038%). Mixtures of (*Z*)-$CF_3CH{=}CHCF_3$ in a He bath gas of between 10 and 35% were prepared manometrically in 12 L Pyrex bulbs for use in the OH rate coefficient measurements. The bulb content was monitored using infrared absorption and found to be stable, to within ~1%, over a period of several weeks.

Gas flows were measured with calibrated electronic mass flow meters and pressures were measured using 10, 100, and 1000 Torr capacitance manometers. The photolysis and probe lasers were operated at 10 Hz repetition rate. The gas flow velocity was in the range of 6−20 cm s^{-1}, ensuring a fresh sample of gas in the LIF reaction volume for each photolysis pulse. The uncertainties quoted herein are at the 2σ (95% confidence) level unless noted otherwise.

3. RESULTS AND DISCUSSION

The rate coefficient results obtained using the PLP−LIF technique for reactions 1 and 2 and the RR technique for reaction 1 are presented separately below. The results are then compared with rate coefficient data for several similar unsaturated fluorinated compounds. Finally, an atmospheric degradation mechanism of (*Z*)-$CF_3CH{=}CHCF_3$ under typical atmospheric conditions as well as its radiative efficiency and GWPs are presented.

3.1. OH and OD Reaction Rate Coefficients Obtained Using PLP−LIF. Rate coefficients for reaction 1 were measured over the temperature range of 212−374 K at pressures between 20 and 200 Torr. A summary of the experimental conditions and the rate coefficients obtained is given in Tables 1 and 2. The rate coefficients were found to be independent of pressure, within the precision of the measurements, at all temperatures included in this study. The OH and OD decay profiles followed pseudo-first-order kinetics, that is, single-exponential decays over at least a 2 orders of magnitude decrease from the initial radical concentration under all experimental conditions. Representative experimental data are provided in the Supporting Information.

Figure 1 shows a summary of the second-order rate coefficient data for reaction 1 obtained at 296 K and the temperature extremes included in this study, 212 and 374 K. The $(k' - k_d)$ values varied linearly with the (*Z*)-$CF_3CH{=}CHCF_3$ concentration over a range of experimental conditions such as $[OH]_0$,

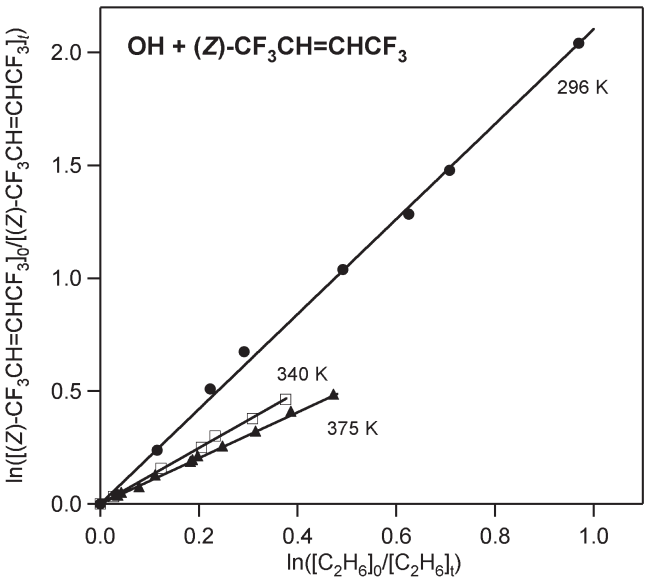

Figure 3. RR data for the OH + (*Z*)-$CF_3CH{=}CHCF_3$ reaction at 296, 345, and 375 K and 100 Torr (He) relative to the OH + C_2H_6 reaction. The lines are least-squares fits of the data yielding the rate coefficient ratios given in Table 3.

photolysis laser fluence, OH radical precursor, and linear gas flow velocity as outlined in Tables 1 and 2. The measured rate coefficients were also found to be independent of O_2 addition to the reaction mixture. In the final analysis, $k_1(T)$ was obtained from a weighted linear least-squares fit of all data obtained at a given temperature, eq I. The fits shown in Figure 1 reproduce the experimental data very well with $k_1(296\ \mathrm{K}) = (4.91 \pm 0.02) \times 10^{-13}$ cm^3 $molecule^{-1}$ s^{-1}, where the quoted uncertainty is from the precision of the fit.

Figure 2 shows the temperature dependence of the measured rate coefficients for reaction 1. $k_1(T)$ has a non-Arrhenius behavior over the temperature range of 212−374 K, where the reaction is nearly independent of temperature between 296 and 374 K but has a weak negative temperature dependence at temperatures below 296 K. $k_1(T)$ is well represented over the entire range of temperatures included in this study using the expression $k_1(T) = AT^2 \exp(-E/RT)$. A linear least-squares fit of the individually measured rate coefficient data given in Table 1, 34 data points, using the expression $\ln(k_1(T)) - 2\ln(T) = \ln(A) - E/RT$ yielded $k_1(T) = (5.73 \pm 0.10) \times 10^{-19} \times T^2 \times \exp[(678 \pm 5)/T]$ cm^3 $molecule^{-1}$ s^{-1}, where the quoted uncertainties are from the precision of the fit. A least-squares fit of the rate coefficient data at temperatures ≤ 300 K to an Arrhenius expression yields $k_1(T < 300\ \mathrm{K}) = (2.63 \pm 0.16) \times 10^{-13} \exp[(185 \pm 15)/T]$ cm^3 $molecule^{-1}$ s^{-1}, where the quoted uncertainties are from the precision of the fit, which would be appropriate for use in atmospheric model calculations.

Rate coefficients for the OD + (*Z*)-$CF_3CH{=}CHCF_3$ (k_2) reaction were measured over the temperature range of 262−374 K. A summary of the experimental conditions and rate coefficients obtained is given in Table 2. Combining all of the results obtained at 296 K yields $k_2(296\ \mathrm{K}) = (5.73 \pm 0.07) \times 10^{-13}$ cm^3 $molecule^{-1}$ s^{-1}, where the quoted uncertainties are from the precision of the fit to eq I. $k_2(T)$ is systematically greater than the rate coefficient obtained for the OH reaction by ∼15%. The larger rate coefficient for the OD reaction is similar to that reported recently from our laboratory for the OH/OD reactions with $CH_2{=}CHF$ and $CH_2{=}CF_2$.[13]

Table 3. Summary of OH + (*Z*)-$CF_3CH{=}CHCF_3$ Reaction Rate Coefficients Obtained in This Work Using a RR Technique

T (K)	reference compound[a]	k_1/k_{ref}[b]	$k_1(T)$[c] (10^{-13} cm^3 $molecule^{-1}$ s^{-1})
296 K	C_2H_6	2.10 ± 0.04	5.25 ± 0.78
		2.04 ± 0.03	5.11 ± 0.77
345 K	C_2H_6	1.24 ± 0.02	4.94 ± 0.89
375 K	C_2H_6	1.02 ± 0.02	5.15 ± 1.29

[a] $k(298\ \mathrm{K}) = 2.5 \times 10^{-13}$ cm^3 $molecule^{-1}$ s^{-1} and $k(T) = 7.66 \times 10^{-12} \exp[-1020/T]$ cm^3 $molecule^{-1}$ s^{-1} for OH + C_2H_6.[9] [b] Quoted uncertainties are at the 2σ level from the precision of the linear least-squares fit of the data. [c] Quoted uncertainties are at the 2σ level and include the 2σ estimated systematic error in the reference reaction rate coefficient.

The temperature dependence of the reaction 2 rate coefficient is similar to that of reaction 1 with $k_2(T) = (4.81 \pm 0.20) \times 10^{-19} \times T^2 \times \exp[(776 \pm 15)/T]$, where the quoted uncertainties are from the precision of the fit. The rate coefficient data for reaction 2 are included in Figure 2 for comparison with the rate coefficients obtained for the OH reaction.

3.2. RR Measurements. Figure 3 shows the results obtained in the RR coefficient measurements for reaction 1 at 296, 345, and 375 K. The loss of (*Z*)-$CF_3CH{=}CHCF_3$ relative to the loss of C_2H_6 obeys eq II to within the precision of the measurements. A linear least-squares fit to the data yielded k_Z/k_{C2H6} values of 2.10 ± 0.04, 1.24 ± 0.02, and 1.02 ± 0.02 at 296, 345, and 375 K, respectively, where the quoted uncertainties are from the precision of the fits. The results of the RR measurements are summarized in Table 3 and included in Figure 2 for comparison with our absolute rate coefficient results. The results obtained using the two techniques agree to within the measurement precision at all temperatures.

3.3. O_3 Reaction Rate Coefficients. The room-temperature (296 K) rate coefficient for the reaction of O_3 with (*Z*)-$CF_3CH{=}CHCF_3$

$$O_3 + (Z)\text{-}CF_3CH{=}CHCF_3 \rightarrow \text{Products} \qquad (7)$$

was measured by monitoring the loss of (*Z*)-$CF_3CH{=}CHCF_3$ in the presence of excess O_3. There was no observable change, <0.5%, in the (*Z*)-$CF_3CH{=}CHCF_3$ concentration in the reactor in the absence of O_3, but under otherwise identical conditions. O_3 loss of as much as 30% was, however, observed over the 1−3 h duration of an experiment, which was also observed under similar conditions in the absence of (*Z*)-$CF_3CH{=}CHCF_3$. An average O_3 concentration was used in the analysis. The experimental data are given in the Supporting Information. We observed an increase in the measured rate coefficient when O_2 was added to the reaction mixture. It should be noted that O_2 was also present in the reactor as an impurity in the O_3 sample, but at a lower concentration than that added directly. The increase of $k_7(296\ \mathrm{K})$ in the presence of O_2 suggests that secondary chemistry possibly played a role under these conditions. In the absence of added O_2, $k_7(296\ \mathrm{K}) = (1.2 \pm 0.3) \times 10^{-21}$ cm^3 $molecule^{-1}$ s^{-1} was obtained from a fit of the (*Z*)-$CF_3CH{=}CHCF_3$ loss to eq I, where the uncertainty is from the precision of the fit. In the

Table 4. Summary of the Rate Coefficient Data for the Reaction of OH with (*Z*)-$CF_3CH{=}CHCF_3$ and Comparison with Rate Coefficients of Structurally Similar Species

compound	k(296 K) (10^{-13} cm^3 molecule^{-1} s^{-1})	$k(T)$ (cm^3 molecule^{-1} s^{-1})	method[a]	pressure range (Torr)	temperature range (K)	reference
(*Z*)-$CF_3CH{=}CHCF_3$	4.91 ± 0.50[b]	$(5.73 \pm 0.60) \times 10^{-19} T^2 \times \exp[(678 \pm 10)/T]$[c]	PLP−LIF	20−200 (He, N_2)	212−374	this work
	5.18 ± 0.46[b]		RR−FTIR	100 (He)	296	this work
$CF_3CF{=}CFCF_3$	4.82 ± 1.15[d]		RR−FTIR	700 (N_2)	296	Young et al.[14]
$CF_3CF{=}CFCF_3$	3.7 ± 0.2[e]		RR−GC	750 (N_2)	298	Cometto et al.[18]
(*Z*)-$CF_3CF{=}CFCF_3$	3.80 ± 0.04	[f]	PLP−RF	30−100 (Ar)	230−370	Orkin et al.[15]
(*E*)-$CF_3CF{=}CFCF_3$	5.86 ± 0.06	[f]	PLP−RF	30−100 (Ar)	230−370	Orkin et al.[15]
(*E*)-$CF_3CH{=}CHF$	9.25 ± 1.72		RR−FTIR	700 (Air)	296	Sondergaard et al.[16]
$CF_3CH{=}CH_2$	15.2 ± 0.5		FP−RF	100 (Ar)	296	Orkin et al.[17]
$CF_3CF_2CF{=}CF_2$	19.4 ± 2.7		RR−FTIR	700 (N_2)	296	Young et al.[14]
$CF_3CF{=}CF_2$	22.1 ± 0.8[g]	$(5.66 \pm 1.4) \times 10^{-13} \times \exp[(407 \pm 85)/T]$[f,g]	FP−RF	100 (Ar)	252−370	Orkin et al.[17]
	21.6 ± 0.7[g]	[f]	FP−RF	30−100 (Ar)	230−480	Orkin et al.[15]
$CH_2{=}CF_2$	27.9 ± 2.5[b]	$(1.75 \pm 0.20) \times 10^{-12} \times \exp[(140 \pm 20)/T]$[c]	PLP−LIF	20−600 (He, N_2)	220−375	Baasandorj et al.[13]
$CH_2{=}CHF$	51.8 ± 5.0[b]	$(1.75 \pm 0.20) \times 10^{-12} \times \exp[(316 \pm 25)/T]$[c]	PLP−LIF	20−600 (He, N_2)	220−375	Baasandorj et al.[13]
$CF_2{=}CF_2$	99.8 ± 1.5[g]	$(3.39 \pm 0.22) \times 10^{-12} \times \exp[(323 \pm 11)/T]$[g]	FP−RF	100 (Ar)	250−370	Orkin et al.[29]

[a] PLP−LIF: pulsed laser photolysis−laser-induced fluorescence; RR−FTIR: relative rate technique using Fourier transform infrared spectroscopy detection; RR−GC: relative rate technique using gas chromatography detection; Rec: recommendation. [b] Uncertainties are at the 2σ level and include estimated systematic errors. [c] The uncertainty in the pre-exponential term includes the estimated systematic errors. The uncertainty in the exponential term is at the 2σ level from the precision of the least-squares fit (rounded off). [d] Reported as the rate coefficient for both (*Z*)- and (*E*)- isomers. [e] Reported rate coefficient obtained using a mixture of isomers. [f] Non-Arrhenius expressions were reported: $2.99 \times 10^{-14} \times (T/298)^{2.61} \times \exp[760/T]$ cm^3 molecule^{-1} s^{-1} for (*Z*)-$CF_3CF{=}CFCF_3$, $7.50 \times 10^{-14} \times (T/298)^{1.68} \times \exp[612/T]$ cm^3 molecule^{-1} s^{-1} for (*E*)-$CF_3CF{=}CFCF_3$, and $9.75 \times 10^{-14} \times (T/298)^{1.94} \times \exp[922/T]$ cm^3 molecule^{-1} s^{-1} for $CF_3CF{=}CF_2$. [g] Uncertainties are at the 2σ level and do not include estimated systematic errors.

presence of 9.7×10^{15} molecules cm^{-3} O_2, k_7(296 K) was found to be $(4.5 \pm 1.2) \times 10^{-21}$ cm^3 molecule^{-1} s^{-1}.

3.4. Error Analysis. Kinetic measurements were carried out over a range of experimental conditions using different bath gases (He, N_2), OH precursors, initial OH concentrations, gas flow velocities, and probe and photolysis laser fluences, as outlined in Tables 1 and 2. The uncertainty in the experimental variables was small, ±1% in pressure, ±2% in flow rate, and ±1 K in temperature. The precision of the measurements was high, with rate coefficients measured under different experimental conditions at a given temperature agreeing to better than 2%.

In the PLP−LIF experiments, the (*Z*)-$CF_3CH{=}CHCF_3$ concentration was determined online using infrared and UV absorption measurements as well as measured gas flows. The three measurements agreed to better than 6% under all experimental conditions. This includes infrared absorption measurements made before and after the LIF reactor that demonstrated no significant loss of the (*Z*)-$CF_3CH{=}CHCF_3$ as it flowed through the apparatus. The uncertainty in the determination of the absorption cross sections was <3%.

A GC analysis of the (*Z*)-$CF_3CH{=}CHCF_3$ sample did not identify any impurities that would significantly influence the rate coefficient measurement. The good agreement in the rate coefficients obtained with the PLP−LIF and RR methods also indicates that sample impurities did not significantly influence the rate coefficient determination at temperatures ≥ 296 K. The absolute uncertainty in the rate coefficient obtained using the RR method was primarily determined by the uncertainty in the reference compound rate coefficient, where the estimated uncertainty in the OH + C_2H_6 reaction rate coefficient is currently estimated to be ∼7% at 298 K and ∼11% at 375 K (1σ).[9]

On the basis of the measurement precision and estimated systematic errors, the overall uncertainty in the absolute rate coefficients is estimated to be ∼9%. The recommended rate coefficients from this work are $k_1(T) = (5.73 \pm 0.60) \times 10^{-19} \times T^2 \times \exp[(678 \pm 5)/T]$ cm^3 molecule^{-1} s^{-1} and $k_2(T) = (4.81 \pm 0.20) \times 10^{-19} \times T^2 \times \exp[(776 \pm 15)/T]$, where the measured room-temperature rate coefficients are k_1(296 K) = $(4.91 \pm 0.50) \times 10^{-13}$ cm^3 molecule^{-1} s^{-1} and k_2(296 K) = $(5.73 \pm 0.50) \times 10^{-13}$ cm^3 molecule^{-1} s^{-1}. The rate coefficient for reaction 1 over the range of temperatures most relevant for atmospheric chemistry can be expressed using an Arrhenius expression as $k_1(T < 300\ \text{K}) = (2.63 \pm 0.40) \times 10^{-13} \exp[(185 \pm 15)/T]$ cm^3 molecule^{-1} s^{-1}. The uncertainty due to estimated systematic errors is included in the pre-exponential terms.

3.5. Rate Coefficient Comparison. To our knowledge, there are no OH radical kinetic studies currently available for hydrofluorobutenes, although studies of the perfluorobutenes $CF_3CF{=}CFCF_3$ and $CF_3CF_2CF{=}CF_2$ have been published.[14,15] Here, we compare the reactivity of (*Z*)-$CF_3CH{=}CHCF_3$ with similarly structured hydrofluoro-olefins and perfluorobutenes.

Table 4 provides a summary of rate coefficient data for several compounds structurally similar to (*Z*)-$CF_3CH{=}CHCF_3$. As with the reaction of OH with olefins, it seems reasonable to assume that reaction 1 proceeds via OH addition to the double bond in (*Z*)-$CF_3CH{=}CHCF_3$. The perfluorinated compounds

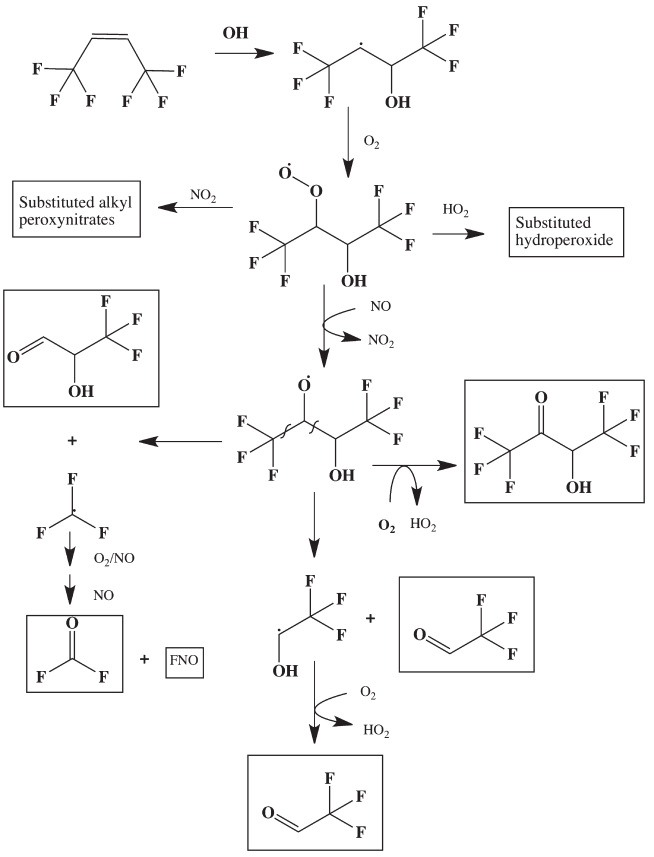

Figure 4. Simplified atmospheric degradation mechanism for (*Z*)-$CF_3CH{=}CHCF_3$ under high NO_x conditions following initiation by reaction with the OH radical. The species enclosed in boxes are the expected stable atmospheric end products.

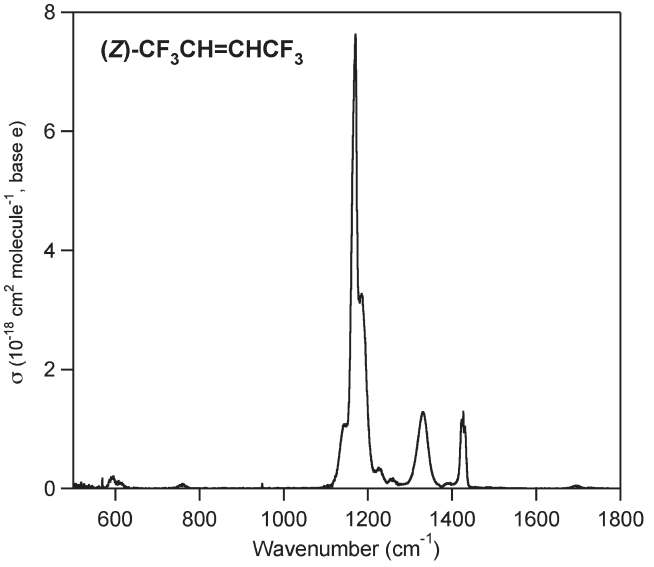

Figure 5. Infrared spectrum (base e) of (*Z*)-$CF_3CH{=}CHCF_3$ measured at 296 K using Fourier transform infrared spectroscopy at 1 cm^{-1} resolution.

$CF_2{=}CF_2$ and $CF_3CF{=}CF_2$ are significantly more reactive toward the OH radical than their partially fluorinated counterparts.[13,15−17] However, the room-temperature rate coefficients for (*Z*)-$CF_3CH{=}CHCF_3$ and (*Z*)-$CF_3CF{=}CFCF_3$[14,15,18] are more similar in magnitude, 4.9×10^{-13} and 3.8×10^{-13} cm^3 $molecule^{-1}$ s^{-1},[15] respectively. (*Z*)-$CF_3CH{=}CHCF_3$ is less reactive than C2−C3 hydrofluoralkenes and $CF_3CF_2CF{=}CF_2$. The decreased OH radical reactivity of the fluorinated 2-butenes is partially the result of fluorine substitution to an olefinic carbon, which leads to a reduction in OH reactivity due to the strong electron-withdrawing effect of fluorine. For example, $CH_2{=}CHF$ and *trans*-$CF_3CH{=}CHF$ are a factor of ∼1.6 less reactive than $CH_2{=}CH_2$ and $CF_3CH{=}CH_2$, respectively. Substitution of a CF_3 group for a F atom on a carbon in the >C=C< bond results in a more pronounced reduction in reactivity, which is attributed to a combination of electron withdrawing as well as steric hindrance by the CF_3 group. For example, a factor of 20 decrease in the 296 K rate coefficient is observed between $CF_2{=}CF_2$,[17,19] $CF_3CF{=}CF_2$,[17] and $CF_3CF{=}CFCF_3$.[14,15] The deactivating effect of the CF_3 group, however, has only been observed for substitution directly at the carbon atom of the >C=C< double bond. Vesine et al.[20] reported that substitution of C_4F_9 or C_6F_{13} groups for the CF_3 group in $CF_3CH{=}CH_2$ did not lead to a significant change in OH reactivity. These qualitative trends in OH reactivity in part explain the difference in reactivity between perfluoro-1-butene and the partially fluorinated 2-butenes.

OH radical reactions with C2 and C3 hydrofluoroalkenes[13,17,20] have a negative temperature dependence over the temperature range of 215−380 K that is consistent with a reaction mechanism involving OH addition to the carbon−carbon double bond. In the present study, $k_1(T)$ was found to have a weak dependence on temperature and a weak non-Arrhenius behavior between 212 and 374 K. The non-Arrhenius behavior is similar to that observed for the reaction of OH with (*Z*)-$CF_3CF{=}CHF$, as reported in a previous study from our laboratory.[6] Non-Arrhenius behavior is sometimes associated with a change of the reaction mechanism, that is, a mechanism dominated by OH radical addition at low temperature with an increasing contribution from H atom abstraction at higher temperatures. However, in the case of reaction, a shift in reaction mechanism is not likely over the limited temperature range included in this study because of the large activation energy associated with the abstraction reaction.[21] Further research is needed to identify the details of the reaction mechanism and its temperature dependence.

4. ATMOSPHERIC IMPLICATIONS

On the basis of the rate coefficients determined in this study, the atmospheric lifetime of (*Z*)-$CF_3CH{=}CHCF_3$ with respect to OH radical reaction is 22 days for an OH concentration of 1×10^6 molecules cm^{-3} using $k_1(272\ K)$.[22] The atmospheric lifetime of (*Z*)-$CF_3CH{=}CHCF_3$ should be considered an approximate value because its actual loss will be highly dependent on the actual time and location of its emission and the associated variations in the OH radical abundance. The O_3 + (*Z*)-$CF_3CH{=}CHCF_3$ reaction rate coefficient at 296 K was found to be $<6 \times 10^{-21}$ cm^3 $molecule^{-1}$ s^{-1}, making atmospheric loss due to reaction with O_3 a minor process (lifetime > 3 years for an O_3 abundance of 50 ppm). The absorption cross section at 253.6 nm determined in this work, $<4 \times 10^{-24}$ cm^2 $molecule^{-1}$, establishes that UV photolysis is a negligible tropospheric loss process for (*Z*)-$CF_3CH{=}CHCF_3$.

An atmospheric degradation mechanism for $CF_3CH{=}CHCF_3$, which is based on analogous well-established hydrocarbon chemistry, under high NO_x conditions is outlined in Figure 4. Under these conditions, the RO_2 radicals formed in the initial steps of the mechanism will primarily react with NO to yield a fluorohydroxyalkoxy (RO) radical or fluorohydroxyperoxynitrate. Unimolecular decomposition of the alkoxy radical via scission of the central carbon−carbon bond leads to the formation of CF_3CHO, while scission of the terminal carbon−carbon bond yields $CF_3CH(OH)CHO$ and CF_2O. Reaction of RO_2 radicals with NO_2 could also lead to the formation of fluoroperoxynitrates. CF_2O, CF_3CHO, CO_2, and CO were the only end products observed in our RR experiments, which were performed under NO_x-free conditions.

In the atmosphere, the $CF_3CH(OH)CHO$ and $CF_3CH(OH)C(O)CF_3$ end products are expected to be short-lived, although no laboratory studies of these species are currently available. CF_2O is removed from the atmosphere primarily via wet deposition and rainout.[4,23] CF_3CHO is removed from the atmosphere by UV photolysis[24,25] (<25 day lifetime) and reaction with OH[25,26] (~20 day lifetime). Therefore, the gas-phase degradation of (*Z*)-$CF_3CH{=}CHCF_3$ is not expected to lead to a significant formation of atmospherically long-lived species.

The photochemical ozone creation potential (POCP) of (*Z*)-$CF_3CH{=}CHCF_3$ was estimated using the method described by Derwent et al.[27] to be 3.4. This is much lower than the POCPs of similar hydrocarbon alkenes, for example, POCPs are 112 for $CH_3CH{=}CH_2$ and 107.9 for $CH_3CH_2CH{=}CH_2$.[27] The contribution of (*Z*)-$CF_3CH{=}CHCF_3$ to regional photochemical ozone formation is, therefore, expected to be small, while the actual contribution would be dependent on its atmospheric abundance.

4.1. Global Warming Potentials (GWPs). The infrared absorption spectrum of (*Z*)-$CF_3CH{=}CHCF_3$ measured in this work at 296 K is given in Figure 5. The (*Z*)-$CF_3CH{=}CHCF_3$ spectrum measured over the concentration range of $(0.70-21.1) \times 10^{14}$ molecules cm^{-3} obeyed Beer's law, varied linearly with concentration, and was independent of bath gas pressure (30−500 Torr, He). Absorption band strengths were determined by a linear least-squares analysis of the integrated absorbance versus [(*Z*)-$CF_3CH{=}CHCF_3$]. Integrated band strengths over the ranges of 1100−1280 and 1280−1500 cm^{-1} were determined to be 21.5 ± 0.12 and 6.26 ± 0.02 (in units of 10^{-17} cm^2 $molecule^{-1}$ cm^{-1}), respectively, where the uncertainties are from the precision of the linear least-squares fit of the integrated absorbance versus concentration. The radiative efficiency (RE) of (*Z*)-$CF_3CH{=}CHCF_3$ was calculated to be 0.38 W m^{-2} ppb^{-1} using the approximation method given by Pinnock et al.[28] For comparison, the RE of (*Z*)-$CF_3CH{=}CHCF_3$ is comparable to that of other unsaturated fluorinated butanes where the RE for $CF_3CF_2CF_2CF_3$ (perfluoro-butane) is 0.33 W m^{-2} ppb^{-1} [1] and that for $CF_3CF{=}CFCF_3$ (perfluoro-2-butene) is 0.32 W m^{-2} ppb^{-1}.[14]

The GWP of (*Z*)-$CF_3CH{=}CHCF_3$ was calculated relative to CO_2 using the lifetimes and radiative efficiencies determined in this study and the integrated radiative forcing of CO_2 given in WMO 2010.[1] The GWPs of (*Z*)-$CF_3CH{=}CHCF_3$ for the 20, 100, and 500 year time horizons are 31, 8.9, and 2.7, respectively, using a (*Z*)-$CF_3CH{=}CHCF_3$ atmospheric lifetime of 22 days.

5. CONCLUSIONS

Rate coefficients for the OH reaction with (*Z*)-$CF_3CH{=}CHCF_3$ were determined over a range of temperatures (212−375 K) and bath gas pressures (20−200 Torr). The rate coefficients were found to be independent of pressure over this range within the precision of the measurements. The measured rate coefficient is well represented by the expression $k_1(T) = (5.73 \pm 0.60) \times 10^{-19} \times T^2 \times \exp[(678 \pm 10)/T]$ cm^3 $molecule^{-1}$ s^{-1}, where the measured room-temperature rate coefficient was $k_1(296\ K) = (4.91 \pm 0.50) \times 10^{-13}$ cm^3 $molecule^{-1}$ s^{-1} and the quoted uncertainties are at the 2σ (95% confidence) level and include estimated systematic errors. The room-temperature rate coefficient for the reaction of O_3 with (*Z*)-$CF_3CH{=}CHCF_3$ was determined to be $<6 \times 10^{-21}$ cm^3 $molecule^{-1}$ s^{-1}. The O_3 reaction represents a minor atmospheric loss process for (*Z*)-$CF_3CH{=}CHCF_3$. On the basis of the OH rate coefficients and infrared spectrum determined in this study, the atmospheric lifetime of (*Z*)-$CF_3CH{=}CHCF_3$ was estimated to be ~20 days, and its global warming potential is ~9 on the 100 year time horizon.

■ ASSOCIATED CONTENT

Supporting Information. Figures of OH radical pseudo-first-order decays, kinetic data for the O_3 + (*Z*)-$CF_3CH{=}CHCF_3$ reaction, and tabulated (*Z*)-$CF_3CH{=}CHCF_3$ infrared cross section data. This material is available free of charge via the Internet at http://pubs.acs.org.

■ AUTHOR INFORMATION

Corresponding Author

*E-mail: [redacted]@noaa.gov.

■ ACKNOWLEDGMENT

We thank Mark Robin and Barbara Minor of DuPont Fluoroproducts for providing the samples and sample purity analysis. This work was supported in part by NOAA's Climate Goal.

■ REFERENCES

(1) *Scientific Assessment of Ozone Depletion: 2010, Global Ozone Research and Monitoring Project*, Report No. 52; World Meteorological Organization (WMO), Geneva, Switzerland, http://ozone.unep.org/Assessment_Panels/SAP/Scientific_Assessment_2010/index.shtml (2011), 516 pp.

(2) *IPCC/TEAP Special Report: Safeguarding the Ozone Layer and the Global Climate System: Issues Related to Hydrofluorocarbons and Perfluorocarbons Institution*; Cambridge University Press: New York, 2005.

(3) *Kyoto Protocol to the United Nations Framework Convention on Climate Change., UNFCCC.* http://unfccc.int/kyoto_protocol/items/2830.php (1997).

(4) Velders, G. J. M.; Fahey, D. W.; Daniel, J. S.; McFarland, M.; Andersen, S. O. *Proc. Natl. Acad. Sci. U.S.A.* **2009**, *106*, 10949–10954.

(5) Davis, M. E.; Gilles, M. K.; Ravishankara, A. R.; Burkholder, J. B. *Phys. Chem. Chem. Phys.* **2007**, *9*, 2240–2248.

(6) Papadimitriou, V. C.; Talukdar, R. K.; Portmann, R. W.; Ravishankara, A. R.; Burkholder, J. B. *Phys. Chem. Chem. Phys.* **2008**, *10*, 808–820.

(7) Papadimitriou, V. C.; Lazarou, Y. G.; Talukdar, R. K.; Burkholder, J. B. *J. Phys. Chem. A* **2011**, *115*, 167–181.

(8) Papadimitriou, V. C.; Portmann, R. W.; Fahey, D. W.; Mühle, J.; Weiss, R. F.; Burkholder, J. B. *J. Phys. Chem. A* **2008**, *112*, 12657–12666.

(9) Sander, S. P.; Abbatt, J.; Barker, J. R.; Burkholder, J. B.; Friedl, R. R.; Golden, D. M.; Huie, R. E.; Kolb, C. E.; Kurylo, M. J.; Moortgat, G. K.; Orkin, V. L.; Wine, P. H. *Chemical Kinetics and Photochemical Data for Use in Atmospheric Studies, Evaluation Number 17*, JPL

Publication 10-6; Jet Propulsion Laboratory, California Institute of Technology: Pasadena, CA, 2011; http://jpldataeval.jpl.nasa.gov.

(10) Baasandorj, M.; Papanastasiou, D. K.; Talukdar, R. K.; Hasson, A. S.; Burkholder, J. B. *Phys. Chem. Chem. Phys.* **2010**, *12*, 12101–12111.

(11) McCabe, D. C.; Rajakumar, B.; Marshall, P.; Smith, I. W. M.; Ravishankara, A. R. *Phys. Chem. Chem. Phys.* **2006**, *8*, 4563–4574.

(12) Rothman, L. S.; Gordon, I. E.; Barbe, A.; Benner, D. C.; Bernath, P. E.; Birk, M.; Boudon, V.; Brown, L. R.; Campargue, A.; Champion, J. P.; Chance, K.; Coudert, L. H.; Dana, V.; Devi, V. M.; Fally, S.; Flaud, J. M.; Gamache, R. R.; Goldman, A.; Jacquemart, D.; Kleiner, I.; Lacome, N.; Lafferty, W. J.; Mandin, J. Y.; Massie, S. T.; Mikhailenko, S. N.; Miller, C. E.; Moazzen-Ahmadi, N.; Naumenko, O. V.; Nikitin, A. V.; Orphal, J.; Perevalov, V. I.; Perrin, A.; Predoi-Cross, A.; Rinsland, C. P.; Rotger, M.; Simeckova, M.; Smith, M. A. H.; Sung, K.; Tashkun, S. A.; Tennyson, J.; Toth, R. A.; Vandaele, A. C.; Vander Auwera, J. *J. Quant. Spectrosc. Radiat. Transfer* **2009**, *110*, 533–572.

(13) Baasandorj, M.; Knight, G.; Papadimitriou, V. C.; Talukdar, R. K.; Ravishankara, A. R.; Burkholder, J. B. *J. Phys. Chem. A* **2010**, *114*, 4619–4633.

(14) Young, C. J.; Hurley, M. D.; Wallington, T. J.; Mabury, S. A. *Atmos. Environ.* **2009**, *43*, 3717–3724.

(15) Orkin, V. L.; Poskrebyshev, G. A.; Kurylo, M. J. *J. Phys. Chem. A* **2011**, *115*, 6568–6574.

(16) Sondergaard, R.; Nielsen, O. J.; Hurley, M. D.; Wallington, T. J.; Singh, R. *Chem. Phys. Lett.* **2007**, *443*, 199–204.

(17) Orkin, V. L.; Huie, R. E.; Kurylo, M. J. *J. Phys. Chem. A* **1997**, *101*, 9118–9124.

(18) Cometto, P. M.; Taccone, R. A.; Nieto, J. D.; Dalmasso, P. R.; Lane, S. I. *ChemPhysChem* **2010**, *11*, 4053–4059.

(19) Acerboni, G.; Jensen, N. R.; Rindone, B.; Hjorth, J. *Chem. Phys. Lett.* **1999**, *309*, 364–368.

(20) Vésine, E.; Bossoutrot, V.; Mellouki, A.; Bras, G. L.; Wenger, J.; Sidebottom, H. *J. Phys. Chem. A* **2000**, *104*, 8512–8520.

(21) Atkinson, R. *Chem. Rev.* **1986**, *86*, 69–201.

(22) Prinn, R. G.; Huang, J.; Weiss, R. F.; Cunnold, D. M.; Fraser, P. J.; Simmonds, P. G.; McCulloch, A.; Harth, C.; Salameh, P.; O'Doherty, S.; Wang, R. H. J.; Porter, L.; Miller, B. R. *Science* **2001**, *292*, 1882–1888.

(23) Wallington, T. J.; Schneider, W. F.; Worsnop, D. R.; Nielsen, O. J.; Sehested, J.; Debruyn, W. J.; Shorter, J. A. *Environ. Sci. Technol.* **1994**, *28*, A320–A326.

(24) Chiappero, M. S.; Malanca, F. E.; Arguello, G. A.; Wooldridge, S. T.; Hurley, M. D.; Ball, J. C.; Wallington, T. J.; Waterland, R. L.; Buck, R. C. *J. Phys. Chem. A* **2006**, *110*, 11944–11953.

(25) Sellevåg, S. R.; Kelly, T.; Sidebottom, H.; Nielsen, C. J. *Phys. Chem. Chem. Phys.* **2004**, *6*, 1243–1252.

(26) Atkinson, R.; Baulch, D. L.; Cox, R. A.; Crowley, J. N.; Hampson, R. F.; Hynes, R. G.; Jenkin, M. E.; Rossi, M. J.; Troe, J. *Atmos. Chem. Phys.* **2006**, *6*, 3625–4055.

(27) Derwent, R. G.; Jenkin, M. E.; Saunders, S. M.; Pilling, M. J. *Atmos. Environ.* **1998**, *32*, 2429–2441.

(28) Pinnock, S.; Hurley, M. D.; Shine, K. P.; Wallington, T. J.; Smyth, T. J. *J. Geophys. Res.* **1995**, *100*, 23227–23238.

(29) Orkin, V. L.; Louis, F.; Huie, R. E.; Kurylo, M. J. *J. Phys. Chem. A* **2002**, *106*, 10195–10199.